

# Supplementary Materials for

## Global trends in biodiversity and ecosystem service from 1900 to 2050

Henrique M. Pereira, Isabel M.D. Rosa, Inês S. Martins, HyeJin Kim, Paul Leadley, Alexander Popp, Detlef P. van Vuuren, George Hurtt, Peter Anthoni, Almut Arneth, Daniele Baisero, Rebecca Chaplin-Kramer, Louise Chini, Fulvio Di Fulvio, Moreno Di Marco, Simon Ferrier, Shinichiro Fujimori, Carlos A. Guerra, Michael Harfoot, Thomas D. Harwood, Tomoko Hasegawa, Vanessa Haverd, Petr Havlík, Stefanie Hellweg, Jelle P. Hilbers, Samantha L. L. Hill, Akiko Hirata, Andrew J. Hoskins, Florian Humpenöder, Jan H. Janse, Walter Jetz, Justin A. Johnson, Andreas Krause, David Leclère, Tetsuya Matsui, Johan R.Meijer, Cory Merow, Michael Obsersteiner, Haruka Ohashi, Benjamin Poulter, Andy Purvis, Benjamin Quesada, Carlo Rondinini, Aafke M. Schipper, Josef Settele, Richard Sharp, Elke Stehfest, Bernardo B. N. Strassburg, Kiyoshi Takahashi, Matthew V. Talluto, Wilfried Thuiller, Nicolas Titeux, Piero Visconti, Christopher Ware, Florian Wolf, Rob Alkemade

Correspondence to: [hpereira@idiv.de](mailto:hpereira@idiv.de)

### **This PDF file includes:**

Materials and Methods  
Figs. S1 to S9  
Tables S1 to S3

## Materials and Methods

This study was conducted under the auspices of the Expert Group on Scenarios and Models of the Intergovernmental Science-Policy Platform on Biodiversity and Ecosystem Services (IPBES). The detailed protocol of this multi-model study was published in (17). Below we summarize the main methodological aspects.

### Scenarios

All models used the same set of scenarios: SSP1 with RCP2.6 (“global sustainability” with low land-use pressure and low level of climate change, (36)), SSP3 with RCP6.0 (“regional rivalry” with high land-use pressure and intermediate level of climate change, (37)), and SSP5 with RCP8.5 (“fossil-fueled development” with intermediate land-use pressure and high level of climate change, (38)) – to assess a broad range of plausible futures (Table S1). We used land-use projections for these scenarios ignoring the impacts of climate change, although the deployment of land-based climate mitigation strategies is considered in connection to each of the SSP-RCP combinations. Land-use projections for SSP3xRCP6.0 were not available, so we chose the closest land-use projections available, SSP3xRCP7.0.

### Land use data

All models used the Land Use Harmonization (39–43) version 2 dataset (LUH2, see <http://luh.umd.edu/data.shtml> for data). LUH2 provides global gridded land-use datasets at 0.25° resolution with annual time-steps comprising estimates of historical land-use change (850-2015) and future projections (2015-2100) under the assumptions of each Shared Socio-economic Pathway (SSP) (44). The 12 land use categories (Table S3) include the separation of primary and secondary natural vegetation into forest and non-forest sub-types, pasture into managed pasture and rangeland, and cropland into multiple crop functional types (C3 annual, C3 perennial, C4 annual, C4 perennial, and C3 nitrogen-fixing crops). The LUH2 dataset also computes all transitions between these 12 land use types, resulting in over 100 possible transitions per grid cell per year (e.g., crop rotations, shifting cultivation, agricultural changes, wood harvest) as well as various agricultural management layers (e.g., irrigation, synthetic nitrogen fertilizer, biofuel crops). Due to specific model parameterizations, each biodiversity and ecosystem service model used its own aggregation of the land use categories (see (17) for more details).

### Climate data

Models used historical climate data and future projections associated with each SSPxRCP combination (20) from CMIP5 / ISIMIP2a (45) or its downscaled version from the WorldClim (46), or the projections from MAGICC 6.0 (47, 48). Most models used the IPSL-CM5A-LR (49) projections which are mid-range across the 5 GCMs in ISIMIP2a (50) – that includes 12 climate variables at 0.5° resolution on daily time steps from the pre-industrial period 1951 to 2099 (45). The WorldClim downscaled dataset has 19 bioclimatic variables monthly from 1960 to 1990 and multi-year averages for specific points in time (e.g., 2050, 2070) up to 2070 at 1km resolution. MAGICC 6.0 climate data (47, 48) in the IMAGE model framework (51) was used for the GLOBIO model.

### Biodiversity models

All models have been published in peer-reviewed journals, although in some cases modifications have been made to the original model (see (17) for details in modifications). In total, 8 spatially-explicit models were used (Table S2), these include three species

distributions models - AIM-biodiversity (52), InSiGHTS (53, 54), MOL (55, 56); and five community models (cSAR-iDiv (57), cSAR-IIASA-ETH (58), BILBI (59), PREDICTS (60, 61), GLOBIO (62, 63). Three of these models, BILBI, PREDICTS and cSAR-iDiv share coefficients for the impacts of land-use on biodiversity from the PREDICTS database (61). The biodiversity models have different methodological approaches, taxonomic groups, spatial resolution and output metrics (Table S2), but they were harmonized as described below.

### Ecosystem services models

For ecosystem functioning and services, five spatially-explicit models were used. They include three process-based DGVM models – LPJ-GUESS (64–66), LPJ (67, 68), and CABLE-POP (69) – and two ecosystem services models – InVEST (70) and GLOBIO-ES (71, 72). These rely on different modelling approaches to estimate a wide range of biophysical outputs, which were harmonized as described in the next sections (see Table S2 for a summary of the models, details available in (17)).

### Scales of analysis (local, regional and global) and harmonization of metrics

Model outputs were produced at three spatial scales: one-degree grid cells ( $\alpha$  metrics), at the regional level (regional  $\gamma$  metrics) for the 17 IPBES sub-regions (73), and at the global level (global  $\gamma$  metrics). The methodology adopted by each modelling team to aggregate from the original resolution of the model to one-degree cells was the arithmetic average of the values in the original resolution.

The model outputs addressed very different facets of biodiversity (e.g., species ranges, local species richness, global species extinctions, abundance-based intactness, and compositional similarity), as well as different facets of ecosystem services (e.g., pollination, carbon sequestration, soil erosion, wood production, nutrient export, coastal vulnerability), often with little overlap between different models. In addition, even for the same facet of biodiversity or ecosystem service, different models outputted different metrics. In order to ensure comparability, output metrics for each model were converted to proportional changes relative to the beginning time of the analysis (e.g.,  $\Delta y = \frac{y_{t1} - y_{t0}}{y_{t0}}$ ), where  $y_t$  is the value of the metric at time  $t$ , and  $t_0$  and  $t_1$  are respectively the beginning and the end of the time period. In addition, models that simulated a continuous time series of climate change impacts calculate  $y_t$  as 20-year averages around the midpoint  $t$  in order to account for inter-annual variability.

### Biodiversity metrics

Outputs of each biodiversity model were assigned to one or more of the following harmonized biodiversity metrics (Table S2): species richness (S), mean species habitat extent ( $\bar{H}$ ), and species-abundance based biodiversity intactness (I). While all metrics were reported as proportional changes relative to the beginning of a time period, intactness was also reported as a score relative to a pristine baseline. For mapping purposes, local changes in proportional species richness were converted in normalized changes in absolute species richness ( $\Delta S$ ), by multiplying by the number of species in each cell divided by the number of species in the richest cell. Global spatial averages of the local metrics were calculated across all terrestrial one-degree cells and are denoted with an overbar (e.g.  $\overline{\Delta S_\alpha}$ ) to distinguish it from averages of a metric across species ( $\bar{H}$ ).

In the end, the harmonized metrics analyzed were:

- $\Delta S_\alpha(x, y) = \frac{S_\alpha(x, y, t1) - S_\alpha(x, y, t0)}{S_\alpha(x, y, t0)}$ , where  $S_\alpha(x, y, t)$  is the number of species at cell (x,y) at time  $t$ ;

- $\Delta S_{\alpha}(x, y) = \Delta S_{\alpha}(x, y) \times \frac{S(x, y)}{\text{Max}_{\{x, y\}}[S(x, y)]}$ , where  $S(x, y)$  is the number of species at cell  $(x, y)$  calculated from current species distribution maps, and the maximum value is calculated across all cells;
- $\Delta S_{\gamma}(\text{region}) = \frac{S_{\gamma}(\text{region}, t1) - S_{\gamma}(\text{region}, t0)}{S_{\gamma}(\text{region}, t0)}$ , where  $S_{\gamma}(\text{region}, t)$  is the number of species in an IPBES sub-region or in the globe at time  $t$ ;
- $\Delta \dot{H}_{\gamma} = \frac{1}{S_{\gamma}} \sum_{i=1}^{S_{\gamma}} \frac{H_{\gamma}(i, t1, i) - H_{\gamma}(i, t0)}{H_{\gamma}(i, t0)}$ , where  $H_{\gamma}(i, t)$  is the global habitat extent of species  $i$  at time  $t$ ;
- $I_{\alpha}(x, y, t)$ , which is the species-abundance based intactness value for cell  $(x, y)$  at time  $t$  relative to a pristine baseline, with 100% corresponding to a pristine habitat and 0% to a completely degraded habitat.

In addition, global spatial averages for  $\alpha$  metrics were calculated as follows:

- $\overline{\Delta S_{\alpha}} = \sum_{x, y} \frac{\Delta S_{\alpha}(x, y)}{n}$
- $\overline{\Delta \dot{H}_{\alpha}} = \sum_{x, y} \frac{\Delta \dot{H}_{\alpha}(x, y)}{n}$
- $\overline{I_{\alpha}} = \sum_{x, y} \frac{I_{\alpha}(x, y)}{n}$

where  $n$  is the number of terrestrial one-degree cells.

The harmonized biodiversity metrics need to be interpreted with care as the original model outputs mapped to the same harmonized metric can differ in some technical details. For instance, the GLOBIO model (62, 63) outputs a metric called “Mean Species Abundance” (MSA) that represents “the mean abundance of original species in relation to a particular pressure as compared to the mean abundance in an undisturbed reference situation”; likewise the PREDICTS model (74) outputs a metric called “Biodiversity Intactness Index (BII)” that represents “the average abundance of originally present species across a broad range of species, relative to abundance in an undisturbed habitat”. While both metrics have been harmonized as representing species-abundance based intactness ( $I$ ), they are calculated differently in the models (i.e., the former is the average of abundance ratios while the latter is the ratio of the sums). Similarly, models based on the species-area relationship (75) produced similar metrics (relative change in species richness) but covered different taxonomic groups (Table S2).

### Ecosystem services metrics

A similar effort was made to assign the metrics outputted by the ecosystem function and services models to a set of harmonized metrics (Table S1). We used the typology of the IPBES Nature’s Contributions to People (NCPs) (19) to classify material and regulating services. For each of the following ecosystem services we assigned one biophysical metric from one or more models, sometimes changing the sign of the reported metric for consistency: bioenergy production; food and feed production; timber production; ecosystem carbon; crop pest control (more is better control); coastal resilience (more is greater resilience); pollination; soil protection; nitrogen retention (more is higher water quality).

The dynamic global vegetation models (DGVMs) tend to output similar metrics and have similar assumptions (76), but the two ecosystem service models (GLOBIO and InVEST) tended to output different metrics for the same service. DGVMs have been used in the climate change modeling community for decades so they benefit from a long history of multi-model inter-comparison (77). Therefore, while for certain metrics, such as ecosystem carbon pool, the metrics are calculated in a similar way and use equivalent biophysical units (e.g. Kg C), for other metrics, e.g., pollination, direct comparison of absolute values was not feasible. For instance, GLOBIO-ES (72, 78) defines their metric of pollination services as

“the fraction of cropland potentially pollinated, relative to all available cropland”, but in InVEST (79) defines it as “the proportion of agricultural lands whose pollination needs are met”. As for biodiversity metrics, this problem was addressed by using proportional changes of each metric in each model at each scale of analysis.

#### Comparison of biodiversity, regulating and material ecosystems services

To understand how biodiversity and ecosystem services varied concurrently in each IPBES sub-region (Figure 4) we mapped regional changes in biodiversity and in aggregated regulating and material ecosystem services, from 2015 to 2050 for all three scenarios. First, we normalized changes in regional species richness ( $\Delta S_{\gamma}$ ) and ecosystem service metrics for all scenarios and regions, by dividing the proportional changes for each sub-region and scenario and model metric by the maximum value of that metric for all subregions in all scenarios. In this way, we obtained a normalized  $\Delta Y$  with values between -1 and +1 for biodiversity or ecosystem service metric in each region and scenario. Next, we clustered all normalized model values into biodiversity metrics, material ecosystem services and regulating ecosystem services.

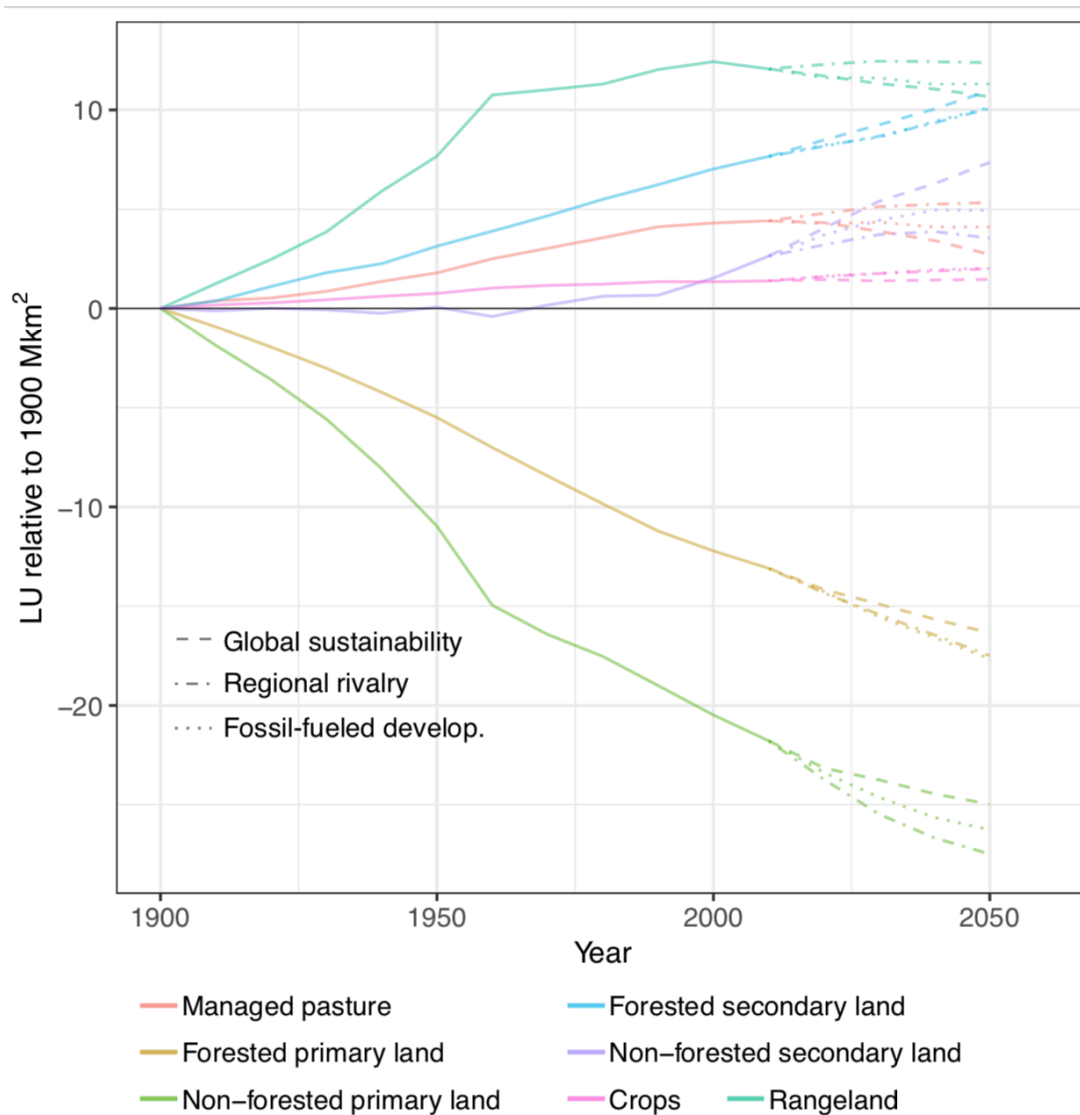
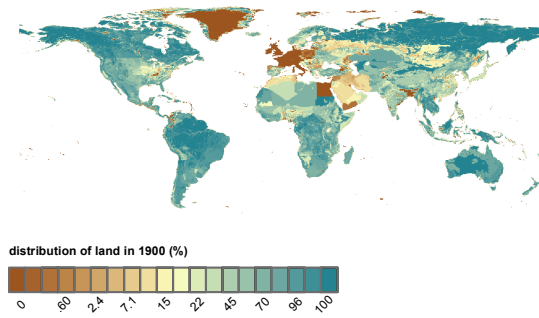
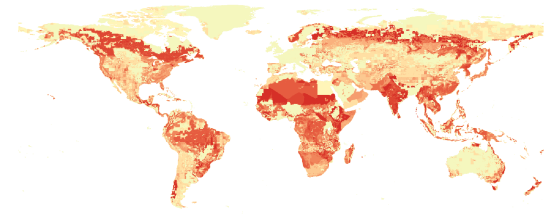


**Fig. S1. (a)** Global historical trends (1990-2015) in land-use and projected trends for each scenario (2015-2050). Lines correspond to absolute area changes relative to the year 1900. The original area covered by each land-use in 1900 was: forested primary land (36.0 Mkm<sup>2</sup>), non-forested primary land (50.7 Mkm<sup>2</sup>), forested secondary land (6.3 Mkm<sup>2</sup>), non-forest secondary land (11.8 Mkm<sup>2</sup>), managed pasture (3.5 Mkm<sup>2</sup>), rangeland (12.9 Mkm<sup>2</sup>), cropland (9.5 Mkm<sup>2</sup>).

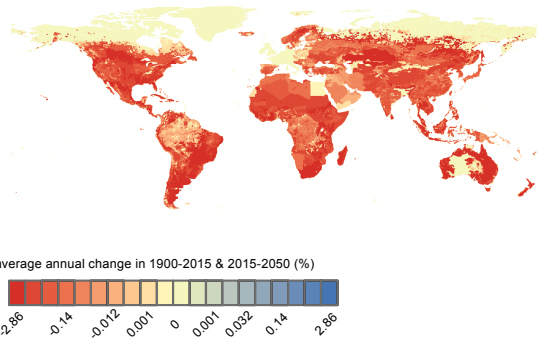
1900



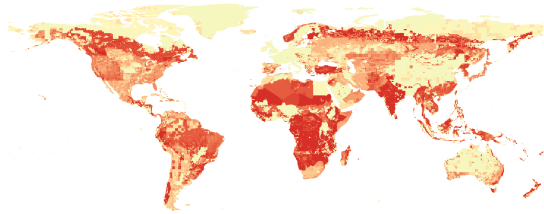
$\Delta$ 2015-2050 - Global sustainability



$\Delta$ 1900-2015



$\Delta$ 2015-2050 - Regional rivalry



$\Delta$ 2015-2050 - Fossil-fueled develop.

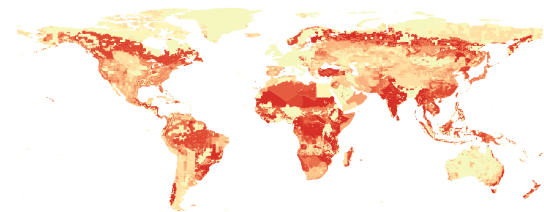
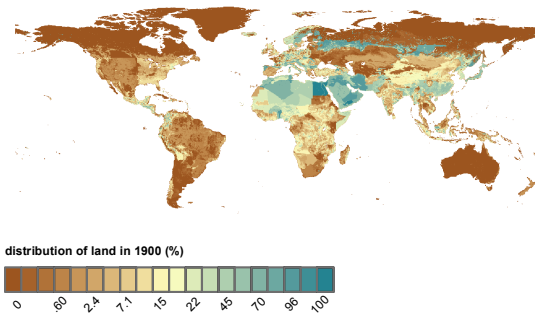
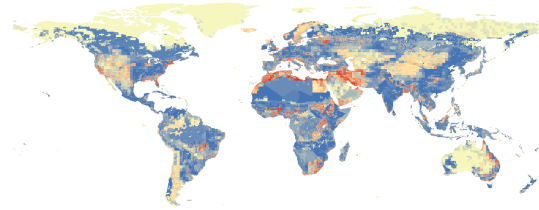


**Figure S1 (b)** Distribution of primary land (forest & non-forest) in 1900, historical changes (1900-2015) and future changes (2015-2050) in each scenario. Please note that changes are reported in absolute percentage points (i.e.,  $y_{t1}-y_{t0}$  where  $y$  is the percentage of the area in a cell covered by that land use type). Color scales are based on quantile intervals considering all land cluster types for i) 1900 and ii) the past ( $\Delta$ 1900-2015) and future ( $\Delta$ 2015-2050) combined.

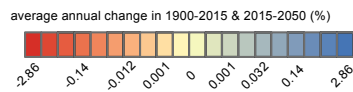
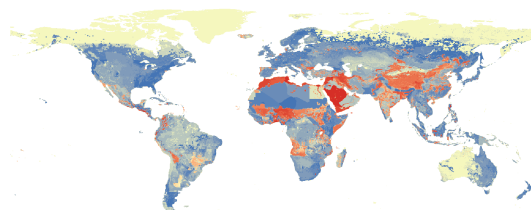
1900



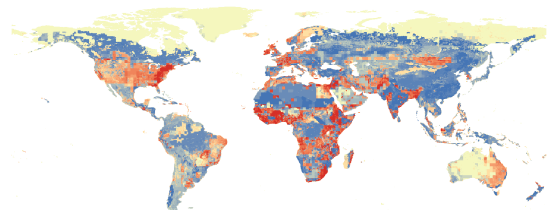
$\Delta$ 2015-2050 - Global sustainability



$\Delta$ 1900-2015



$\Delta$ 2015-2050 - Regional rivalry



$\Delta$ 2015-2050 - Fossil-fueled develop.

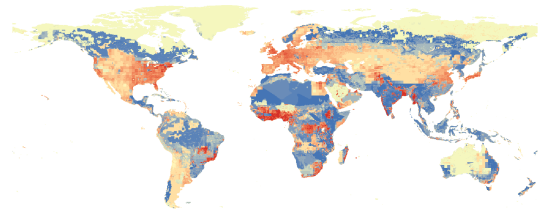
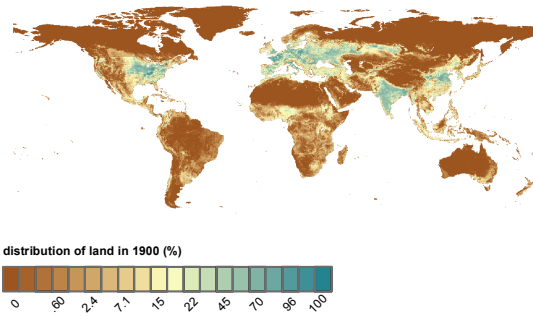
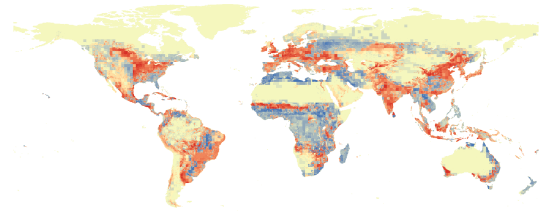


**Figure S1 (c)** Distribution of secondary land (forest & non-forest) in 1900, historical changes (1900-2015) and future changes (2015-2050) in each scenario. Please note that changes are reported in absolute percentage points (i.e.  $y_{t1}-y_{t0}$  where  $y$  is the percentage of the area in a cell covered by that land use type). Color scales are based on quantile intervals considering all land cluster types for i) 1900 and ii) the past ( $\Delta$ 1900-2015) and future ( $\Delta$ 2015-2050) combined.

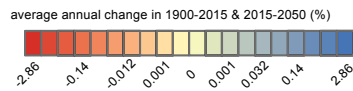
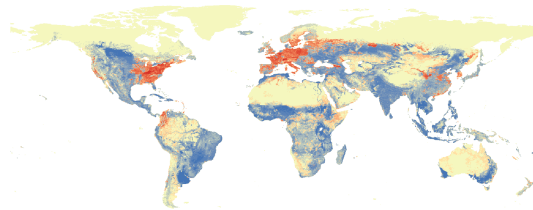
1900



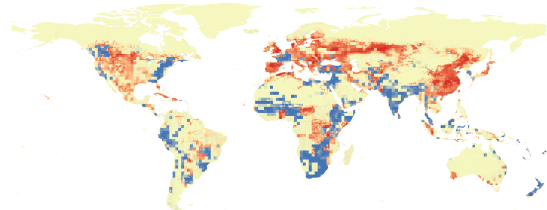
$\Delta$ 2015-2050 - Global sustainability



$\Delta$ 1900-2015



$\Delta$ 2015-2050 - Regional rivalry



$\Delta$ 2015-2050 - Fossil-fueled develop.

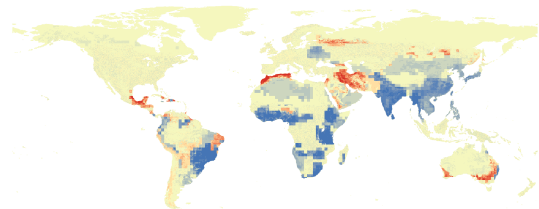
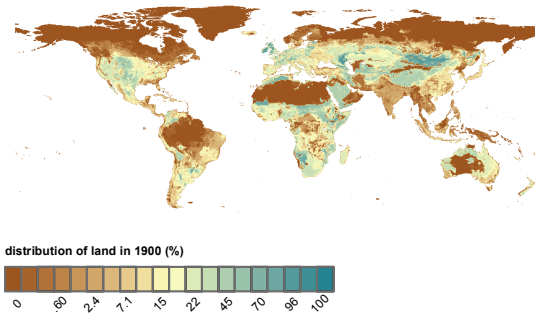
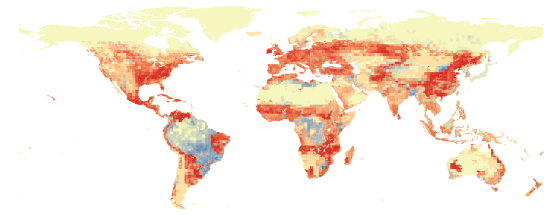


**Figure S1 (d)** Distribution of cropland (C3 & C4) in 1900, historical changes (1900-2015) and future changes (2015-2050) in each scenario, in percentage. Please note that changes are reported in absolute percentage points (i.e.  $y_{t1}-y_{t0}$  where  $y$  is the percentage of the area in a cell covered by that land use type). Color scales are based on quantile intervals considering all land cluster types for i) 1900 and ii) the past ( $\Delta$ 1900-2015) and future ( $\Delta$ 2015-2050) combined.

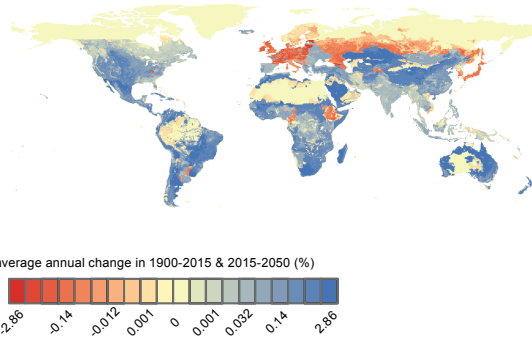
1900



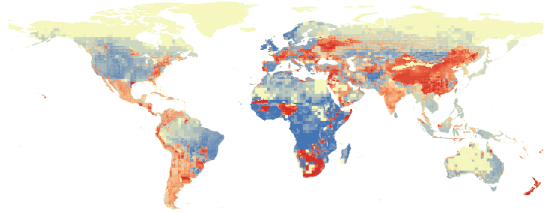
$\Delta$ 2015-2050 - Global sustainability



$\Delta$ 1900-2015



$\Delta$ 2015-2050 - Regional rivalry



$\Delta$ 2015-2050 - Fossil-fueled develop.

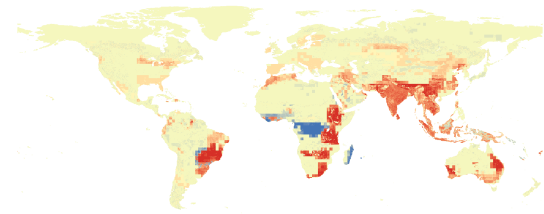


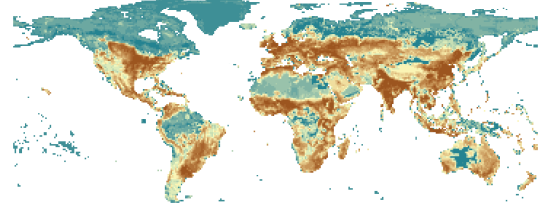
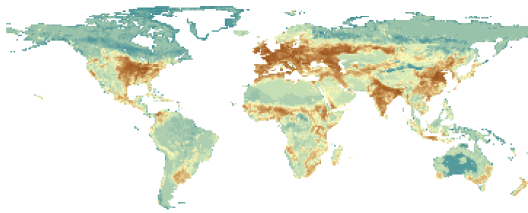
**Figure S1 (e)** Distribution of pasture and rangeland in 1900, historical changes (1900-2015) and future changes (2015-2050) in each scenario, in percentage. Please note that changes are reported in absolute percentage points (i.e.  $y_{t1}-y_{t0}$  where  $y$  is the percentage of the area in a cell covered by that land use type). Color scales are based on quantile intervals considering all land cluster types for i) 1900 and ii) the past ( $\Delta$ 1900-2015) and future ( $\Delta$ 2015-2050) combined.



each scenario (2015-2050): **(b)** global sustainability - RCP2.6, **(c)** regional rivalry - RCP6.0, **(d)** fossil-fueled development - RCP8.5.

(a) Historical (1900)

(b) Historical (2050)



(c) Fossil-fueled develop. - LU (2050)

(d) Fossil-fueled develop. - LUCC (2050)

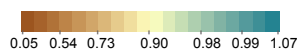
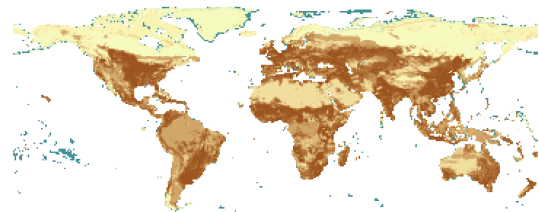
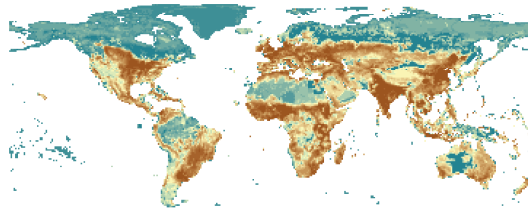
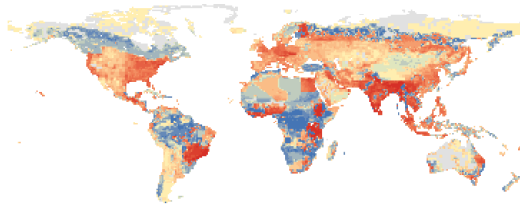
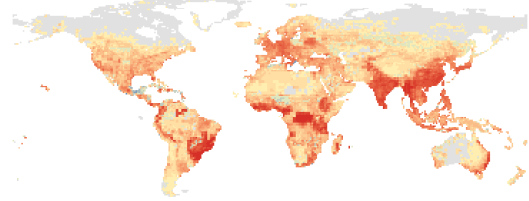


**Fig. S3.** Spatial distribution of intactness ( $I$ ): **(a)** year 1900; **(b)** 2015; **(c-d)** 2050 in the fossil-fueled development scenario based on land-use change alone **(c)** and on the combined impacts of land-use change and climate **(d)**. Values correspond to the inter-model mean between PREDICTS and GLOBIO, except for **(d)** which is based only on GLOBIO. Values are scores relative to a pristine baseline (a score of 1 corresponds to pristine, while a score of 0 corresponds to fully degraded). Color scale is based on quantile intervals when considering all maps features.

(a) cSAR-iDiv



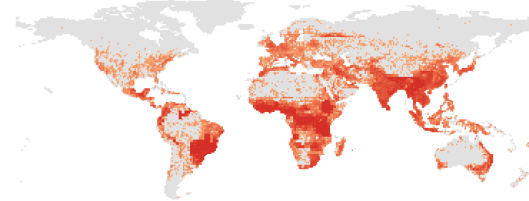
(b) cSAR-IIASA-ETH



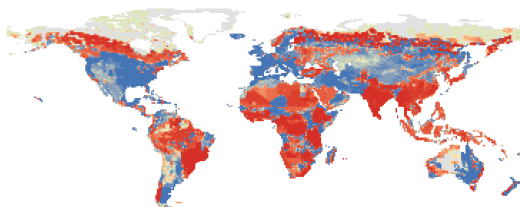
(c) InSIGHTS



(d) AIM



(e) PREDICTS



(f) Intermodel mean

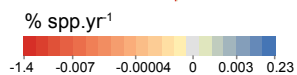
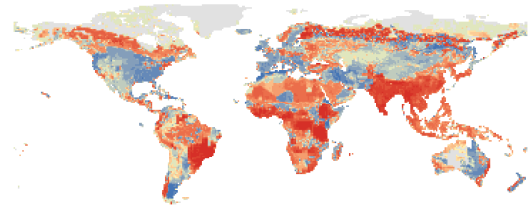


**Fig. S4.** Spatial agreement between biodiversity models. Projection of normalized changes in local species richness per year ( $\Delta SS_{\alpha}$ ) during 2015-2050 caused by land-use change alone for the regional rivalry scenario: **(a)** cSAR-iDiv model; **(b)** cSAR-IIASA-ETH model; **(c)** InSIGHTS model; **(d)** AIM-B model; **(e)** PREDICTS model; **(f)** inter-model mean. A value of 1% yr<sup>-1</sup> corresponds to a decline in the number of local species equal to 1% species of the most speciose grid cell. Color scale is based on quantile intervals when considering all maps features.

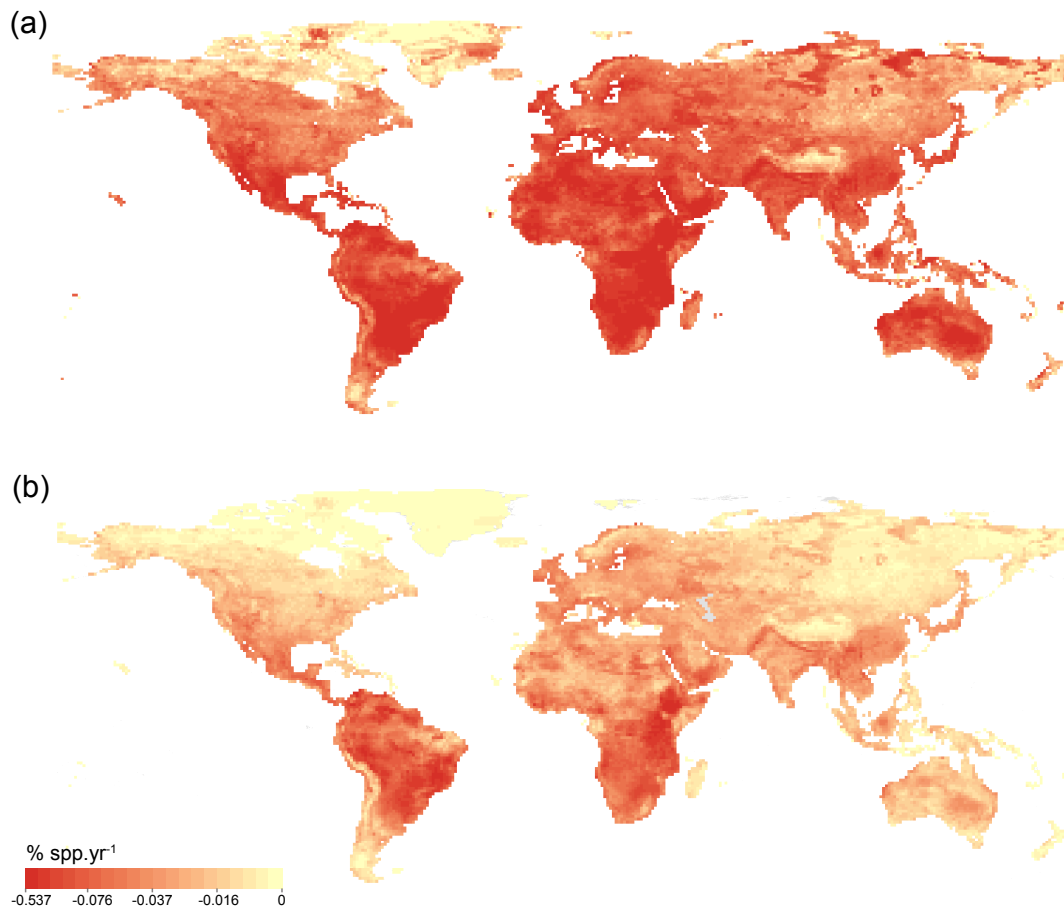
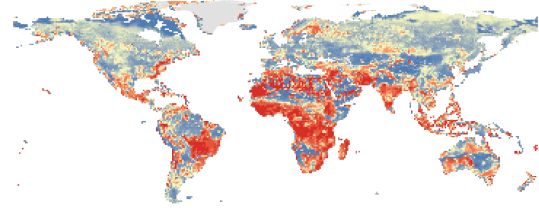
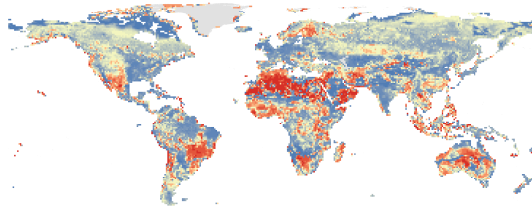


**Fig. S5.** Biodiversity metrics of the AIM model for the fossil fueled development scenario for 2015-2050: **(a)** proportional changes in local species richness ( $\Delta S_\alpha$ ); **(b)** normalized changes in local species richness per year ( $\Delta SS_\alpha$ ). Color scale is based on quantile intervals when considering all maps features.

(a) Global sustainability

(b) Regional rivalry



(c) Fossil-fueled develop.

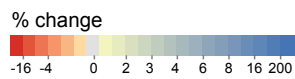
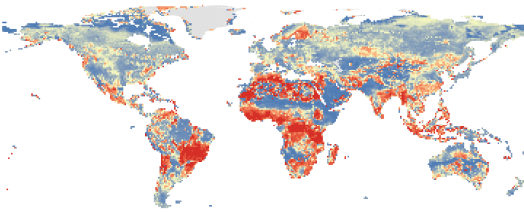
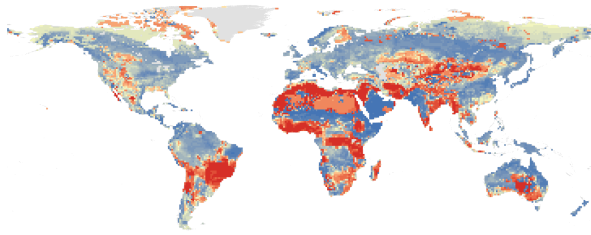
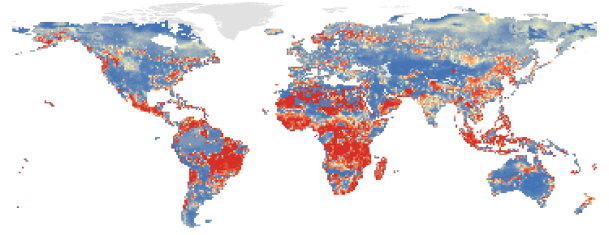


**Fig. S6.** Ecosystem carbon pools across scenarios. Inter-model mean of proportional changes for 2015-2050 (N=4, CABLE-POP, LPJ, LPJ-GUESS, GLOBIO-ES): (a) global sustainability, (b) regional rivalry, (c) fossil-fueled development. Color scale is based on quantile intervals when considering all maps features.

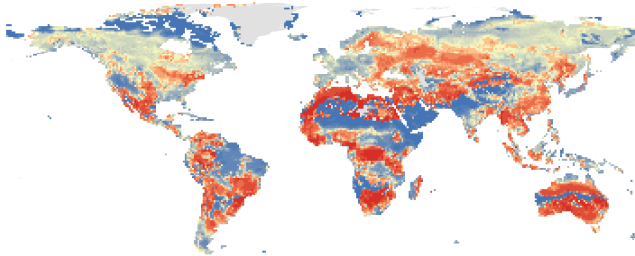
(a) CABLE



(b) GLOBIO-ES



(c) LPJ



(d) LPJ-GUESS

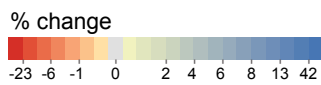
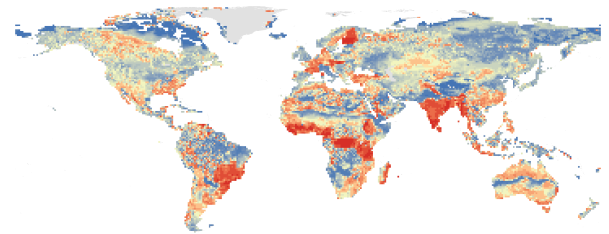
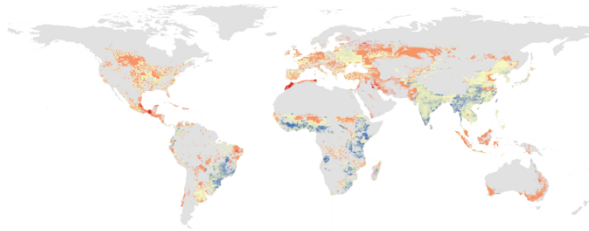
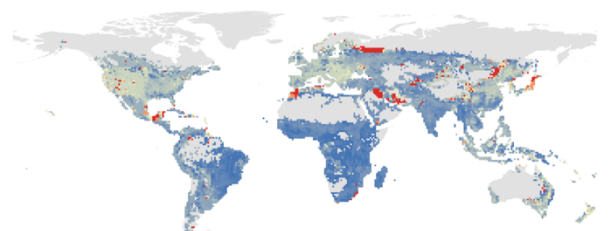


**Fig. S7.** Spatial agreement across models in ecosystem carbon for the fossil fuel development scenario for 2015-2050: **(a)** CABLE-POP, **(b)** GLOBIO-ES, **(c)** LPJ and **(d)** LPJ-GUESS. The inter-model mean can be found in Figure S7. Color scale is based on quantile intervals when considering all maps features.

(a) InVEST



(b) GLOBIO-ES



(c) LPJ-GUESS

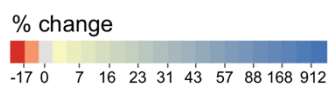
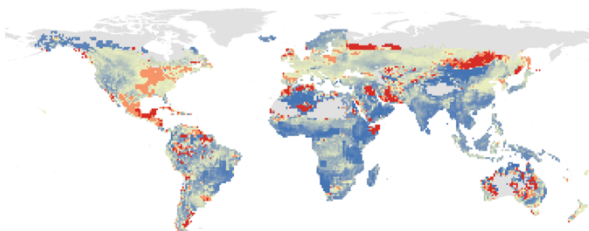
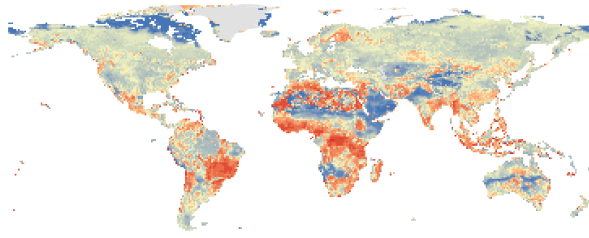
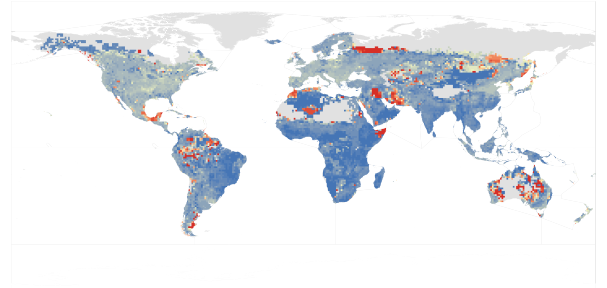


**Fig. S8.** Spatial agreement across models in modelled food and feed production for the fossil fueled development scenario for 2015-2050: **(a)** InVEST, **(b)** GLOBIO-ES and **(c)** LPJ-GUESS. The inter-model mean can be found in Figure S7. Color scale is based on quantile intervals when considering all maps features.

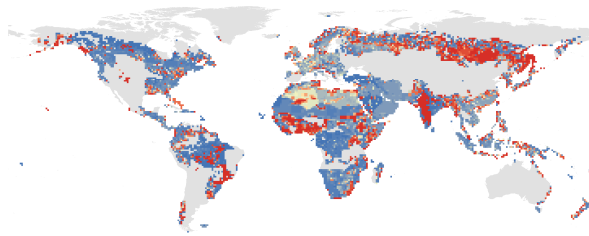
(a) Ecosystem carbon



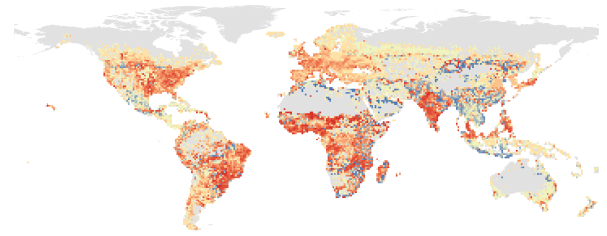
(b) Food and feed production



(c) Timber production



(d) Crop pollination



(e) Nitrogen retention

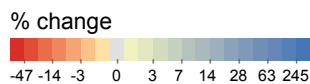
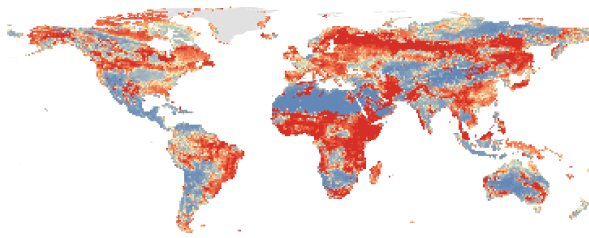


**Fig. S9.** Spatial distribution of ecosystem service changes. Inter-model mean projection of proportional changes (2015-2050) in the fossil fueled development scenario for: (a) Ecosystem carbon (N=4), (b) Food and feed production (N=3), (c) Timber production (N=2), (d) Crop pollination (N=2) and (e) Nitrogen retention (N=2). Colour scale is based on quantile intervals when considering all maps features.

**Table S1.** Characteristics of SSP and RCP scenarios (based on (18) and <https://secure.iiasa.ac.at/web-apps/ene/SspDb/dsd?Action=htmlpage&page=about>)

	SSP1xRCP2.6 Global sustainability	SSP3xRCP6.0 Regional Rivalry	SSP5 Fossil-fueled Development
Land-use projections			
Population growth	Relatively low (8.5 billion in 2050)	Low to high (10 billion in 2050)	Relatively low (8.5 billion in 2050)
Economic growth	High to medium (284,565 GDP/PPP billion US\$2005/yr in 2050)	Slow (177,284 GDP/PPP billion US\$2005/yr in 2050)	High (360,926 GDP/PPP billion US\$2005/yr in 2050)
Urbanization	High (92% in 2050)	Low (60% in 2050)	High (92% in 2050)
Equity and social cohesion	High	Low	High
International trade and globalization	Moderate	Strongly constrained	High
Policy focus	Sustainable development	Security	Development, free market, human capital
Institution effectiveness	Effective	Weak	Increasingly effective
Technology development	Rapid	Slow	Rapid
Land-use regulation	Strong	Limited	Medium
Agricultural productivity	High	Low	High
Consumption & diet	Low growth, low-meat	Resource-intensive	Material-intensive, meat- rich diet
Mitigation policies in land use	Full	Absent	Absent
Bioenergy	High	Low	Lowest
Climate projections			
Carbon intensity	Low	High	High
Energy intensity	Low	Intermediate	High
Radiative forcing	Peak at 3W/m <sup>2</sup> before 2100 and declines	Stabilizes to 6W/m <sup>2</sup> in 2100	Rising to 8.5 W/m <sup>2</sup> in 2100
Concentration (p.p.m)	Peak at 490 CO <sub>2</sub> equiv. before 2100 then declines	850 CO <sub>2</sub> equiv. (at stabilization after 2100)	>1,370 CO <sub>2</sub> equiv. in 2100
Methane emissions	Reduced	Stable	Rapid increase

**Table S2. Model description, metrics, and scenarios**

Model	Description	Taxonomic scope	Metrics	Scenarios
AIM-biodiversity (Asia-Pacific Integrated Model – biodiversity)	A species distribution model that estimates biodiversity loss based projected shift of species range under the conditions of land-use and climate change. Species range shifts were projected under two commonly used dispersal assumptions: 'no' migration, which did not allow for species colonization and 'full' migration, which allowed for species colonization. Only the "no-migration" estimates were used.	Amphibians, birds, mammals, plants, reptiles	$S\alpha$ $S\gamma$ $H\gamma$	Historical Land use Land use and climate
InSiGHTS	A high-resolution, cell-wise, species-specific hierarchical species distribution model that estimate the extent of suitable habitat (ESH) for mammals accounting for land and climate suitability. The model did not consider species colonization in this exercise.	Mammals	$S\alpha$ $S\gamma$ $H\gamma$	Historical Land use Land use and climate
MOL (Map of Life)	An expert map based species distribution model that projects potential losses in species occurrences and geographic range sizes given changes in suitable conditions of climate and land cover change. The model considered range loss within the currently known distribution, and not the species colonization in this exercise.	Amphibians, birds, mammals	$S\alpha$ $S\gamma$ $H\gamma$	Land use and climate
cSAR (Countryside Species Area Relationship) - iDiv	A countryside species-area relationship model that estimates the number of species persisting in a human-modified landscape, accounting for the habitat preferences of different species groups.	Birds	$S\alpha$ $S\gamma$	Historical Land use
cSAR-IIASA-ETH	A countryside species area relationship model that estimates the impact of time series of spatially explicit land-use and land-cover changes on community-level measures of terrestrial biodiversity.	Amphibians, birds, mammals, plants, reptiles	$S\alpha$ $S\gamma$	Historical Land use
<i>BILBI</i> (Biogeographic modelling Infrastructure for Large-scale Biodiversity Indicators)	A modelling framework that couples application of the species-area relationship with correlative generalized dissimilarity modeling (GDM)-based modelling of continuous patterns of spatial and temporal turnover in the species composition of communities (applied in this study to vascular plant species globally).	Vascular plants	$S\gamma$	Historical Land use Land use and climate

Model	Description	Taxonomic scope	Metrics	Scenarios
PREDICTS (Projecting Responses of Ecological Diversity In Changing Terrestrial Systems)	The hierarchical mixed-effects model that estimates how four measures of site-level terrestrial biodiversity – overall abundance, within-sample species richness, abundance-based compositional similarity and richness-based compositional similarity – respond to land use and related pressures.	All	$S\alpha$ $I\alpha$	Historical Land use
GLOBIO	A modelling framework that quantifies the impacts of multiple anthropogenic pressures on biodiversity intactness, quantified as the mean species abundance (MSA) metric.	All	$I\alpha$	Historical Land use Land use and climate
LPJ-GUESS (Lund-Potsdam-Jena General Ecosystem Simulator)	A big leaf model that simulates the coupled dynamics of biogeography, biogeochemistry and hydrology under varying climate, atmospheric CO <sub>2</sub> concentrations, and land-use land cover change practices to represent demography of grasses and trees in a scale from individuals to landscapes.	Not applicable	Bioenergy production Food and feed production Ecosystem carbon Nitrogen retention	Historical Land use Land use and climate
LPJ (Lund-Potsdam-Jena)	A big leaf model that simulates the coupled dynamics of biogeography, biogeochemistry and hydrology under varying climate, atmospheric CO <sub>2</sub> concentrations, and land-use land cover change practices to represent demography of grasses and trees in a scale from individuals to landscapes.	Not applicable	Ecosystem carbon	Historical Land use Land use and climate
CABLE-POP (Community Atmosphere Biosphere Land Exchange)	A “demography enabled” global terrestrial biosphere model that computes vegetation and soil state and function dynamically in space and time in response to climate change, land-use change, CO <sub>2</sub> concentrations and N-input.	Not applicable	Ecosystem carbon Timber production	Historical Land use Land use and climate
GLOBIO-E S	The model simulates the influence of various anthropogenic drivers on ecosystem functions and services.	Not applicable	Crop pest control Nitrogen retention	Land use and climate
InVEST (Integrated Valuation of Ecosystem Services and Tradeoffs)	A suite of geographic information system (GIS) based spatially-explicit models used to map and value the ecosystem goods and services in biophysical or economic terms.	Not applicable	Coastal resilience Pollination Nitrogen retention	Historical Land use and climate

**Table S3. Description of land use categories in LUH2 (based on (39, 42, 80))**

forested primary land (primf)	natural vegetation that has never been impacted by human activities (agriculture or wood harvesting) and that is potentially forest; there is no transition to primary land from any other land cover categories
non-forested primary land (primn)	natural vegetation that has never been impacted by human activities (agriculture or wood harvesting) and is non-forest based on the LUH2 potential forest land layer; there is no transition to primary land from any other land cover categories
potentially forested secondary land (secdf)	natural vegetation that is recovering from previous human disturbance (either wood harvesting or agricultural abandonment) and is potentially forest; secondary land can never return to primary land
potentially non-forested secondary land (secdn)	natural vegetation that is recovering from previous human disturbance (either wood harvesting or agricultural abandonment) and is potentially non-forest; secondary land can never return to primary land
managed pasture (pastr)	land where livestock is known to be grazed regularly or permanently with some level of management activities, with low aridity and high population density
rangeland (range)	land where livestock is known to be grazed regularly or permanently, with high aridity and low population density; not managed except by grazing (i.e., no external inputs of pesticides or fertilizers, or fire/mowing)
urban land (urban)	areas with human habitation and/or buildings where primary vegetation has been removed
C3 annual crops (c3ann)	land where native vegetation has been removed and replaced with C3 annual crops; includes biofuel crops
C3 perennial crops (c3per)	land where native vegetation has been removed and replaced with C3 perennial crops; includes biofuel crops
C4 annual crops (c4ann)	land where native vegetation has been removed and replaced with C4 annual crops; includes biofuel crops
C4 perennial crops (c4per)	land where native vegetation has been removed and replaced with C4 perennial crops; includes biofuel crops
C3 nitrogen-fixing crops (c3nfx)	land where native vegetation has been removed and replaced with C3 nitrogen fixing crops; includes biofuel crops

## References

36. D. P. van Vuuren, E. Stehfest, D. E. H. J. Gernaat, J. C. Doelman, M. van den Berg, M. Harmsen, H. S. de Boer, L. F. Bouwman, V. Daioglou, O. Y. Edelenbosch, B. Girod, T. Kram, L. Lassaletta, P. L. Lucas, H. van Meijl, C. Müller, B. J. van Ruijven, S. van der Sluis, A. Tabeau, Energy, land-use and greenhouse gas emissions trajectories under a green growth paradigm. *Global Environmental Change*. **42**, 237–250 (2017).
37. S. Fujimori, T. Hasegawa, T. Masui, K. Takahashi, D. S. Herran, H. Dai, Y. Hijioka, M. Kainuma, SSP3: AIM implementation of Shared Socioeconomic Pathways. *Global Environmental Change*. **42**, 268–283 (2017).
38. E. Kriegler, N. Bauer, A. Popp, F. Humpenöder, M. Leimbach, J. Strefler, L. Baumstark, B. L. Bodirsky, J. Hilaire, D. Klein, I. Mouratiadou, I. Weindl, C. Bertram, J.-P. Dietrich, G. Luderer, M. Pehl, R. Pietzcker, F. Piontek, H. Lotze-Campen, A. Biewald, M. Bonsch, A. Giannousakis, U. Kreidenweis, C. Müller, S. Rolinski, A. Schultes, J. Schwanitz, M. Stevanovic, K. Calvin, J. Emmerling, S. Fujimori, O. Edenhofer, Fossil-fueled development (SSP5): An energy and resource intensive scenario for the 21st century. *Global Environmental Change*. **42**, 297–315 (2017).
39. G. C. Hurtt, L. P. Chini, S. Frohking, R. A. Betts, J. Feddema, G. Fischer, J. P. Fisk, K. Hibbard, R. A. Houghton, A. Janetos, C. D. Jones, G. Kindermann, T. Kinoshita, K. Klein Goldewijk, K. Riahi, E. Shevliakova, S. Smith, E. Stehfest, A. Thomson, P. Thornton, D. P. van Vuuren, Y. P. Wang, Harmonization of land-use scenarios for the period 1500–2100: 600 years of global gridded annual land-use transitions, wood harvest, and resulting secondary lands. *Climatic Change*. **109**, 117–161 (2011).
40. G. Hurtt, L. Chini, R. Sahajpal, S. Frohking, B. L. Bodirsky, K. Calvin, J. Doelman, J. Fisk, S. Fujimori, K. K. Goldewijk, T. Hasegawa, P. Havlik, A. Heinemann, F. Humpenöder, J. Jungclaus, J. Kaplan, T. Krisztin, D. Lawrence, P. Lawrence, O. Mertz, J. Pongratz, A. Popp, K. Riahi, E. Shevliakova, E. Stehfest, P. Thornton, D. van Vuuren, X. Zhang, Harmonization of Global Land Use Change and Management for the Period 850-2015 (2019), , doi:10.22033/ESGF/input4MIPs.10454.
41. G. Hurtt, L. Chini, R. Sahajpal, S. Frohking, B. L. Bodirsky, K. Calvin, J. Doelman, J. Fisk, S. Fujimori, K. K. Goldewijk, T. Hasegawa, P. Havlik, A. Heinemann, F. Humpenöder, J. Jungclaus, J. Kaplan, T. Krisztin, D. Lawrence, P. Lawrence, O. Mertz, J. Pongratz, A. Popp, K. Riahi, E. Shevliakova, E. Stehfest, P. Thornton, D. van Vuuren, X. Zhang, Harmonization of Global Land Use Change and Management for the Period 2015-2300 (2019), , doi:10.22033/ESGF/input4MIPs.10468.
42. K. Klein Goldewijk, A. Beusen, J. Doelman, E. Stehfest, New anthropogenic land use estimates for the Holocene; HYDE 3.2. *Earth System Science Data Discussions*, 1–40 (2016).
43. C. Monfreda, N. Ramankutty, J. A. Foley, *Global Biogeochemical Cycles*, in press, doi:10.1029/2007GB002947.
44. A. Popp, K. Calvin, S. Fujimori, P. Havlik, F. Humpenöder, E. Stehfest, B. L. Bodirsky, J. P. Dietrich, J. C. Doelmann, M. Gusti, T. Hasegawa, P. Kyle, M. Obersteiner, A. Tabeau, K. Takahashi, H. Valin, S. Waldhoff, I. Weindl, M. Wise, E. Kriegler, H.

- Lotze-Campen, O. Fricko, K. Riahi, D. P. van Vuuren, Land-use futures in the shared socio-economic pathways. *Global Environmental Change*. **42**, 331–345 (2017).
45. C. F. McSweeney, R. G. Jones, How representative is the spread of climate projections from the 5 CMIP5 GCMs used in ISI-MIP? *Climate Services*. **1**, 24–29 (2016).
  46. S. E. Fick, R. J. Hijmans, WorldClim 2: new 1-km spatial resolution climate surfaces for global land areas: NEW CLIMATE SURFACES FOR GLOBAL LAND AREAS. *International Journal of Climatology*. **37**, 4302–4315 (2017).
  47. M. Meinshausen, S. C. B. Raper, T. M. L. Wigley, Emulating coupled atmosphere-ocean and carbon cycle models with a simpler model, MAGICC6 – Part 1: Model description and calibration. *Atmospheric Chemistry and Physics*. **11**, 1417–1456 (2011).
  48. M. Meinshausen, T. M. L. Wigley, S. C. B. Raper, Emulating atmosphere-ocean and carbon cycle models with a simpler model, MAGICC6 – Part 2: Applications. *Atmospheric Chemistry and Physics*. **11**, 1457–1471 (2011).
  49. J. L. Dufresne, M. A. Foujols, S. Denvil, A. Caubel, O. Marti, O. Aumont, Y. Balkanski, S. Bekki, H. Bellenger, R. Benshila, S. Bony, L. Bopp, P. Braconnot, P. Brockmann, P. Cadule, F. Cheruy, F. Codron, A. Cozic, D. Cugnet, N. de Noblet, J.-P. Duvel, C. Ethé, L. Fairhead, T. Fichefet, S. Flavoni, P. Friedlingstein, J.-Y. Grandpeix, L. Guez, E. Guilyardi, D. Hauglustaine, F. Hourdin, A. Idelkadi, J. Ghattas, S. Joussaume, M. Kageyama, G. Krinner, S. Labetoulle, A. Lahellec, M.-P. Lefebvre, F. Lefevre, C. Levy, Z. X. Li, J. Lloyd, F. Lott, G. Madec, M. Mancip, M. Marchand, S. Masson, Y. Meurdesoif, J. Mignot, I. Musat, S. Parouty, J. Polcher, C. Rio, M. Schulz, D. Swingedouw, S. Szopa, C. Talandier, P. Terray, N. Viovy, N. Vuichard, Climate change projections using the IPSL-CM5 Earth System Model: from CMIP3 to CMIP5. *Climate Dynamics*. **40**, 2123–2165 (2013).
  50. L. Warszawski, K. Frieler, V. Huber, F. Piontek, O. Serdeczny, J. Schewe, The Inter-Sectoral Impact Model Intercomparison Project (ISI-MIP): Project framework. *Proceedings of the National Academy of Sciences*. **111**, 3228–3232 (2014).
  51. E. Stehfest, D. van Vuuren, T. Kram, L. Bouwman, R. Alkemade, M. Bakkenes, R. Biemans, A. F. Bouwman, M. den Elzen, J. H. Janse, P. Lucas, J. van Minnen, M. Müller, A. Prins, *Integrated Assessment of Global Environmental Change with IMAGE 3.0. Model description and policy applications* (PBL Netherlands Environmental Assessment Agency, The Hague, 2014).
  52. H. Ohashi, T. Hasegawa, A. Hirata, S. Fujimori, K. Takahashi, I. Tsuyama, K. Nakao, Y. Kominami, N. Tanaka, Y. Hijioka, T. Matsui, Biodiversity can benefit from climate stabilization despite adverse side effects of land-based mitigation. *Nature Communications* (in press).
  53. C. Rondinini, M. Di Marco, F. Chiozza, G. Santulli, D. Baisero, P. Visconti, M. Hoffmann, J. Schipper, S. N. Stuart, M. F. Tognelli, G. Amori, A. Falcucci, L. Maiorano, L. Boitani, Global habitat suitability models of terrestrial mammals. *Philosophical Transactions of the Royal Society B: Biological Sciences*. **366**, 2633–2641 (2011).

54. P. Visconti, M. Bakkenes, D. Baisero, T. Brooks, S. H. M. Butchart, L. Joppa, R. Alkemade, M. Di Marco, L. Santini, M. Hoffmann, L. Maiorano, R. L. Pressey, A. Arponen, L. Boitani, A. E. Reside, D. P. van Vuuren, C. Rondinini, Projecting Global Biodiversity Indicators under Future Development Scenarios: Projecting biodiversity indicators. *Conservation Letters*. **9**, 5–13 (2016).
55. W. Jetz, D. S. Wilcove, A. P. Dobson, Projected Impacts of Climate and Land-Use Change on the Global Diversity of Birds. *PLoS Biology*. **5**, e157 (2007).
56. C. Merow, M. J. Smith, J. A. Silander, A practical guide to MaxEnt for modeling species' distributions: what it does, and why inputs and settings matter. *Ecography*. **36**, 1058–1069 (2013).
57. I. S. Martins, H. M. Pereira, Improving extinction projections across scales and habitats using the countryside species-area relationship. *Scientific Reports*. **7** (2017), doi:10.1038/s41598-017-13059-y.
58. A. Chaudhary, F. Verones, L. de Baan, S. Hellweg, Quantifying Land Use Impacts on Biodiversity: Combining Species–Area Models and Vulnerability Indicators. *Environmental Science & Technology*. **49**, 9987–9995 (2015).
59. M. Di Marco, T. D. Harwood, A. J. Hoskins, C. Ware, S. L. L. Hill, S. Ferrier, Projecting impacts of global climate and land-use scenarios on plant biodiversity using compositional-turnover modelling. *Global Change Biology*. **25**, 2763–2778 (2019).
60. T. Newbold, L. N. Hudson, A. P. Arnell, S. Contu, A. De Palma, S. Ferrier, S. L. L. Hill, A. J. Hoskins, I. Lysenko, H. R. P. Phillips, V. J. Burton, C. W. T. Chng, S. Emerson, D. Gao, G. Pask-Hale, J. Hutton, M. Jung, K. Sanchez-Ortiz, B. I. Simmons, S. Whitmee, H. Zhang, J. P. W. Scharlemann, A. Purvis, Has land use pushed terrestrial biodiversity beyond the planetary boundary? A global assessment. *Science*. **353**, 288–291 (2016).
61. A. Purvis, T. Newbold, A. De Palma, S. Contu, S. L. L. Hill, K. Sanchez-Ortiz, H. R. P. Phillips, L. N. Hudson, I. Lysenko, L. Börger, J. P. W. Scharlemann, in *Advances in Ecological Research* (Elsevier, 2018; <http://linkinghub.elsevier.com/retrieve/pii/S0065250417300284>), vol. 58, pp. 201–241.
62. R. Alkemade, M. van Oorschot, L. Miles, C. Nellemann, M. Bakkenes, B. ten Brink, GLOBIO3: A Framework to Investigate Options for Reducing Global Terrestrial Biodiversity Loss. *Ecosystems*. **12**, 374–390 (2009).
63. A. M. Schipper, J. P. Hilbers, J. R. Meijer, L. H. Antão, A. Benítez-López, M. M. J. Jonge, L. H. Leemans, E. Scheper, R. Alkemade, J. C. Doelman, S. Mylius, E. Stehfest, D. P. Vuuren, W. Zeist, M. A. J. Huijbregts, *Glob Change Biol*, in press, doi:10.1111/gcb.14848.
64. M. Lindeskog, A. Arneth, A. Bondeau, K. Waha, J. Seaquist, S. Olin, B. Smith, Implications of accounting for land use in simulations of ecosystem carbon cycling in Africa. *Earth System Dynamics*. **4**, 385–407 (2013).

65. S. Olin, G. Schurgers, M. Lindeskog, D. Wårlind, B. Smith, P. Bodin, J. Holmér, A. Arneth, Modelling the response of yields and tissue C : N to changes in atmospheric CO<sub>2</sub> and N management in the main wheat regions of western Europe. *Biogeosciences*. **12**, 2489–2515 (2015).
66. B. Smith, D. Wårlind, A. Arneth, T. Hickler, P. Leadley, J. Siltberg, S. Zaehle, Implications of incorporating N cycling and N limitations on primary production in an individual-based dynamic vegetation model. *Biogeosciences*. **11**, 2027–2054 (2014).
67. B. Poulter, D. C. Frank, E. L. Hodson, N. E. Zimmermann, Impacts of land cover and climate data selection on understanding terrestrial carbon dynamics and the CO<sub>2</sub> airborne fraction. *Biogeosciences*. **8**, 2027–2036 (2011).
68. S. Sitch, B. Smith, I. C. Prentice, A. Arneth, A. Bondeau, W. Cramer, J. O. Kaplan, S. Levis, W. Lucht, M. T. Sykes, K. Thonicke, S. Venevsky, Evaluation of ecosystem dynamics, plant geography and terrestrial carbon cycling in the LPJ dynamic global vegetation model. *Global Change Biology*. **9**, 161–185 (2003).
69. V. Haverd, B. Smith, L. Nieradzick, P. R. Briggs, W. Woodgate, C. M. Trudinger, J. G. Canadell, M. Cuntz, A new version of the CABLE land surface model (Subversion revision r4601) incorporating land use and land cover change, woody vegetation demography, and a novel optimisation-based approach to plant coordination of photosynthesis. *Geoscientific Model Development*. **11**, 2995–3026 (2018).
70. R. Sharp, H. T. Tallis, T. Ricketts, A. D. Guerry, S. A. Wood, R. Chaplin-Kramer, E. Nelson, D. Ennaanay, S. Wolny, N. Olwero, K. Vigerstol, D. Pennington, G. Mendoza, J. Aukema, J. Foster, J. Forrest, D. Cameron, K. Arkema, E. Lonsdorf, C. Kennedy, G. Verutes, C. K. Kim, G. Guannel, M. Papenfus, J. Toft, M. Marsik, J. Bernhardt, R. Griffin, K. Glowinski, N. Chaumont, N. Perelman, M. Lacayo, L. Mandle, P. Hamel, A. L. Vogl, L. Rogers, W. Bierbower, D. Denu, J. Douglass, *InVEST + VERSION+ User's Guide, The Natural Capital Project* (Stanford University, University of Minnesota, The Nature Conservancy, and World Wildlife Fund, 2016).
71. R. Alkemade, B. Burkhard, N. D. Crossman, S. Nedkov, K. Petz, Quantifying ecosystem services and indicators for science, policy and practice. *Ecological Indicators*. **37**, 161–162 (2014).
72. C. J. E. Schulp, R. Alkemade, K. Klein Goldewijk, K. Petz, Mapping ecosystem functions and services in Eastern Europe using global-scale data sets. *International Journal of Biodiversity Science, Ecosystem Services & Management*. **8**, 156–168 (2012).
73. T. M. Brooks, H. R. Akçakaya, N. D. Burgess, S. H. M. Butchart, C. Hilton-Taylor, M. Hoffmann, D. Juffe-Bignoli, N. Kingston, B. MacSharry, M. Parr, L. Perianin, E. C. Regan, A. S. L. Rodrigues, C. Rondinini, Y. Shennan-Farpon, B. E. Young, Analysing biodiversity and conservation knowledge products to support regional environmental assessments. *Scientific Data*. **3** (2016), doi:10.1038/sdata.2016.7.
74. T. Newbold, L. N. Hudson, S. L. L. Hill, S. Contu, I. Lysenko, R. A. Senior, L. Börger, D. J. Bennett, A. Choimes, B. Collen, J. Day, A. De Palma, S. Díaz, S. Echeverria-Londoño, M. J. Edgar, A. Feldman, M. Garon, M. L. K. Harrison, T. Alhusseini, D. J.

- Ingram, Y. Itescu, J. Kattge, V. Kemp, L. Kirkpatrick, M. Kleyer, D. L. P. Correia, C. D. Martin, S. Meiri, M. Novosolov, Y. Pan, H. R. P. Phillips, D. W. Purves, A. Robinson, J. Simpson, S. L. Tuck, E. Weiher, H. J. White, R. M. Ewers, G. M. Mace, J. P. W. Scharlemann, A. Purvis, Global effects of land use on local terrestrial biodiversity. *Nature*. **520**, 45–50 (2015).
75. H. M. Pereira, G. C. Daily, Modeling Biodiversity Dynamics in Countryside Landscapes. *Ecology*. **87**, 1877–1885 (2006).
76. A. Quillet, C. Peng, M. Garneau, Toward dynamic global vegetation models for simulating vegetation–climate interactions and feedbacks: recent developments, limitations, and future challenges. *Environmental Reviews*. **18**, 333–353 (2010).
77. C. Prudhomme, I. Giuntoli, E. L. Robinson, D. B. Clark, N. W. Arnell, R. Dankers, B. M. Fekete, W. Franssen, D. Gerten, S. N. Gosling, S. Hagemann, D. M. Hannah, H. Kim, Y. Masaki, Y. Satoh, T. Stacke, Y. Wada, D. Wisser, Hydrological droughts in the 21st century, hotspots and uncertainties from a global multimodel ensemble experiment. *Proceedings of the National Academy of Sciences*. **111**, 3262–3267 (2014).
78. R. S. de Groot, R. Alkemade, L. Braat, L. Hein, L. Willemen, Challenges in integrating the concept of ecosystem services and values in landscape planning, management and decision making. *Ecological Complexity*. **7**, 260–272 (2010).
79. H. Tallis, S. Polasky, Mapping and Valuing Ecosystem Services as an Approach for Conservation and Natural-Resource Management. *Annals of the New York Academy of Sciences*. **1162**, 265–283 (2009).
80. S. L. L. Hill, R. Gonzalez, K. Sanchez-Ortiz, E. Caton, F. Espinoza, T. Newbold, J. Tylianakis, J. P. W. Scharlemann, A. De Palma, A. Purvis, Worldwide impacts of past and projected future land-use change on local species richness and the Biodiversity Intactness Index. *bioRxiv* (2018), doi:10.1101/311787.